

# STATUS OF THE SILICON STRIP VERTEX DETECTOR FOR THE MARK II EXPERIMENT AT THE SLC\*

CHRIS ADOLPHSEN, GIORGIO GRATTA<sup>†</sup>, ALAN LITKE,  
ANDREAS SCHWARZ AND MICHAL TURALA<sup>†</sup>

*Santa Cruz Institute for Particle Physics  
University of California, Santa Cruz, CA 95064*

ALAN BREAKSTONE AND SHERWOOD PARKER

*University of Hawaii, Honolulu, HI 96822*

BRUCE BARNETT, PAUL DAUNCEY AND DAVID DREWER

*Johns Hopkins University, Baltimore, MD 21218*

and

ROBERT JACOBSEN AND VERA LÜTH

*Stanford Linear Accelerator Center  
Stanford University, Stanford, California, 94305*

## Abstract

We are constructing a silicon strip vertex detector to be used in the Mark II detector in the study of  $Z^0$  decays at the SLAC Linear Collider. The status of the project, including the performance of the individual silicon detector modules, is presented.

## Introduction

The Mark II detector will be the first to run at the SLAC Linear Collider (SLC) which is presently undergoing commissioning. We are building a silicon strip vertex detector (SSVD) for this experiment to enhance the study of short lived particles produced in  $Z^0$  decays. The SLC provides an excellent setting for the use of a SSVD in a number of ways. The small beam spot ( $\sigma_{z,y} = 2\mu\text{m}$ ;  $\sigma_z = 1\text{mm}$ ) essentially eliminates the interaction point uncertainty while the small beam pipe radius (2.6 cm) allows for a compact detector and reduces the multiple scattering contribution to the impact parameter resolution. Also, the low beam crossing frequency (120 Hz) permits a high density of channels since power to the analog read-out electronics can be switched off between pulses.

Given the space constraints within the Mark II detector, we settled for a SSVD design with three detector layers that cover 77% of the solid angle from the interaction point (see figure 1). The detectors measure position only in the  $r - \phi$  plane; the Mark II central tracking chamber provides the  $z$  information. The three layers insure that every track has at least two hits

in the SSVD which is useful for track finding especially if background rates are high. There are 12 detectors per layer and 512 strips per detector giving a total of about 18,000 channels. The read-out of such a high density of strips has become possible in the last few years with the production of a custom VLSI chip ("Microplex") of 128 channels that is roughly  $6 \times 6 \text{ mm}^2$  [1]. The fabrication technology is NMOS using  $5 \mu\text{m}$  design rules. The circuit integrates and stores (double correlated sampling) the charge deposited on a strip and can multiplex the analog signal onto a serial bus. Another development which simplified the implementation of this project is the fabrication of detectors on four inch diameter silicon wafers [2]. This allows us to span a solid angle comparable to the central tracking chamber using only one detector length. The properties of the detectors are given in table 1.

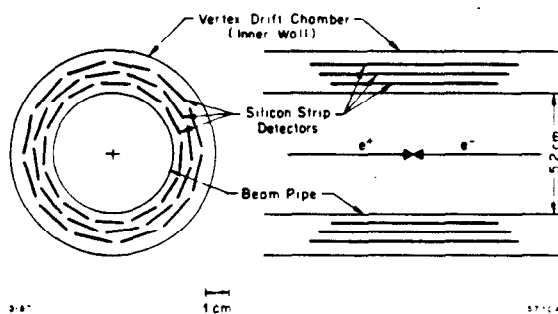


Figure 1. The layout of the Silicon Strip Vertex Detector.

\* Work supported by the Department of Energy, Contracts DE-AC03-76SF-00515, DE-AA03-76SF00034, and DE-AC03-83ER-40103 and the National Science Foundation Grant 87 01 610

<sup>†</sup> Fellow of Istituto Nazionale di Fisica, Rome, Italy.

<sup>†</sup> Visitor from the Institute of Nuclear Physics, Krakow, Poland.

## Beam Tests

To determine the signal characteristics of detectors with Microplex readout, we first built three fixed target style modules that were run in a 15 GeV positron beam [3]. The detector strips were 60 mm long, had 25  $\mu\text{m}$  pitch and were wire bonded

Table 1

Properties of the Silicon Detectors

Detector Property	layer 1	layer 2	layer 3	units
layer radius	30	34	38	mm
strip pitch	25	29	33	$\mu\text{m}$
number of strips	512	512	512	
active length	72	82	90	mm
total length	75	85	94	mm
active width	13	15	17	mm
total width	14	16	18	mm
thickness	300	300	300	$\mu\text{m}$
strip width	8	8	8	$\mu\text{m}$
depletion voltage	$\sim 50$	$\sim 50$	$\sim 50$	V
capacitance* (to other strips)	8.2	8.8	9.3	pF
capacitance* (to backplane)	0.6	0.8	1.0	pF

\* calculated.

to version 2 of the Microplex chip. For the beam at normal incidence to the detector, the most probable energy loss signal was 17 times the average strip noise for the detector with the narrowest strip width ( $10 \mu\text{m}$ ). In this case, the cuts used to find hits yielded essentially 100% efficiency for the beam signal while noise events occurred less than  $10^{-5}$  per strip per trigger. The position resolution was better than  $5 \mu\text{m}$  in each case and two tracks could be resolved using a simple finding algorithm to within a separation of  $150 \mu\text{m}$  without loss of efficiency or spatial resolution.

### Vertex Resolution

Although a  $5 \mu\text{m}$  SSVD resolution provides a high accuracy point near the beam axis, the track angle is still better determined from the large radial separation of measurements in the central drift chamber of the Mark II. Considering the intrinsic resolutions of the tracking detectors in the Mark II including the SSVD, and the multiple scattering contribution from materials of the detectors and beam pipe, the impact parameter resolution can be derived. The result is shown as a

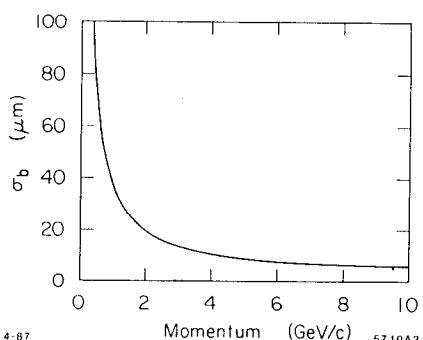


Figure 2. Impact parameter resolution ( $\sigma_b$ ) as a function of momentum for tracks produced at  $90^\circ$  to the beam axis.

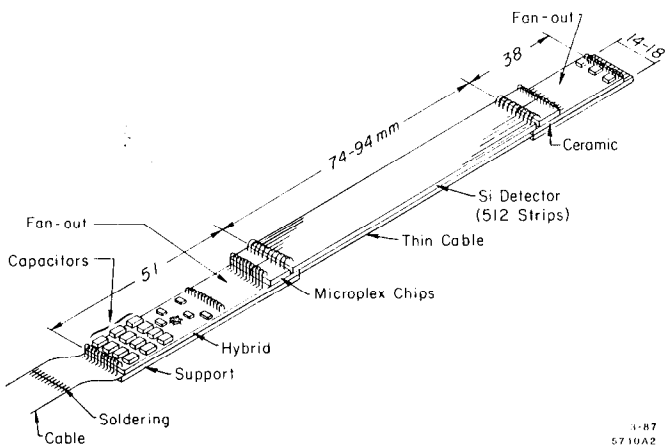


Figure 3. The plan for a silicon detector module.

function of track momentum in figure 2. This resolution will give good tagging efficiency for  $B$  meson decays, for example, where the average secondary track momentum is a few  $\text{GeV}/c$  and the mean impact parameter is about  $200 \mu\text{m}$ .

### Detector Modules

Since the beam tests, we have constructed a number of prototype detector assemblies that will be compatible with the space requirements of the Mark II. As shown in figure 3, the modules consist of a detector with two read-out chips wire bonded on each end that process every other channel. The Microplex chips are epoxied onto a hybrid circuit which provides the control lines, a switchable capacitor bank for the power, and a differential amplifier and line driver for the analog output signals. Flexible cables are used to bring the signals from the outside to either ends of the module and from the hybrid to the read-out chip. The outside cables are brought in along the beam pipe from only one end of the Mark II detector to avoid ground loop problems and make the SSVD installation easier. The output analog signals are sent to an intelligent digitizer, the BADC [4], which we are programming to do on-line pedestal subtraction and updating, common mode correction, and hit finding.

The Microplex chips we are currently using are version 3 which have been fabricated to cure problems with version 2 as well as to improve its performance. The new chips have lower noise and consume less power ( $14 \text{ mW}/\text{channel}$  analog and  $.63 \text{ mW}/\text{channel}$  digital). The amplifier rise time is about  $25 \text{ nsec}$  and we generally use a  $500 \text{ nsec}$  integration period. The equivalent noise charge (ENC) of Microplex 3 as a function of the external input capacitance is shown in figure 4. This data were taken with a chip in which surface mount capacitors were wire bonded to the input pads. The data points have a normalization uncertainty of about 10%. It should be noted that the strip noise spectrum adheres very well to a Gaussian distribution out to the limits of the data at five sigma.

One potential problem with using Microplex 3 is that the signal to noise ratio drops by a factor of two after about  $20 \text{ krad}$  of radiation exposure independent of whether the chip is powered or not [5]. Since it is still not clear what the background radiation environment of the SSVD will be at the SLC,

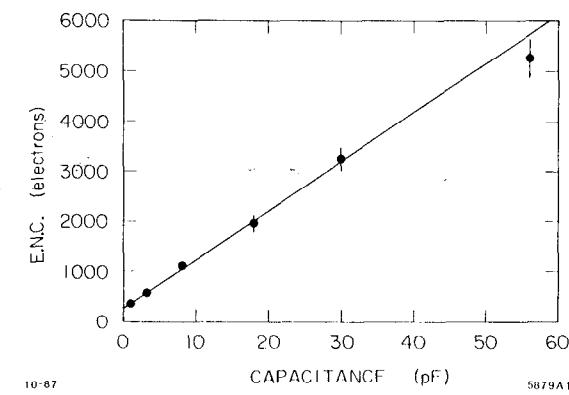


Figure 4. The equivalent charge noise (ENC) of Microplex 3 as a function of external input capacitance. The line fit to the data has an intercept of 280 electrons and a slope of 97 electrons/pF.

especially during beam tuning, we would like the electronics to be as radiation hard as possible. Consequently, we are planning another fabrication of the Microplex chip with changes geared toward improving its survival under radiation exposure.

The silicon strip detectors we will use are much more radiation resistant and show a  $\approx 90 \text{ nA}$  increase in leakage current per  $\text{Mrad}$  exposure ( $> 400 \text{ nA}$  saturates the amplifier). Limits on the initial leakage currents have been guaranteed by the manufacturer as has the maximum voltage for full depletion (75 V). At 10 V above the measured depletion value, the leakage currents should be smaller than  $20 \text{ nA}$  for more than 97% of the strips and not more than  $20 \mu\text{A}$  in total. Also, no more than two strips can have currents above  $200 \text{ nA}$ . These specifications should be readily achievable given that ten of the last twelve detector prototypes we tested each have less than two strips with leakage currents above  $20 \text{ nA}$  and all pass the depletion voltage requirement. Figure 5 shows an example of a depletion measurement for one of the 90 mm long detectors.

Limits on detector thickness (280 to 320  $\mu\text{m}$ ) have also been met with the prototypes although only half pass a requirement that they are flat to 15  $\mu\text{m}$ . The concern here is that an

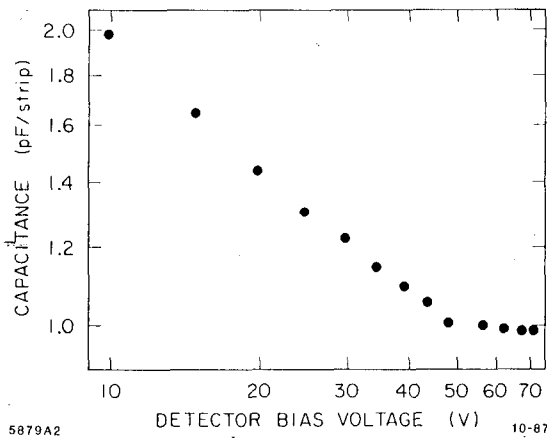


Figure 5. The strip to backplane capacitance as a function of the bias voltage for a 90 mm long detector. The leveling off of the data at about 50 V corresponds to full depletion of the detector.

aplanarity translates into a  $\phi$  error for tracks passing through the detector at angles other than normal incidence (the maximum slope of tracks originating from the interaction point is about .2). However, the largest deviation from planarity for each detector is less than  $24 \mu\text{m}$  and the bowing shape that is observed allows for a simple geometrical correction to be applied when determining location of the hits.

### Module Performance

To estimate the signal-to-noise ratio we can expect for minimum ionizing particles with our modules, we are measuring signals from 60 keV X-rays produced from a 250 mCi  $^{241}\text{Am}$  source. These signals correspond to 71% of the most probable energy loss of minimum ionizing particles in 300  $\mu\text{m}$  silicon. The photo-electrons produced from the X-ray absorption have a range less than 20  $\mu\text{m}$  and so the collected charge is spread among the strips in a distribution similar to that from minimum ionizing radiation.

In analysing the X-ray data, a gain correction is made per strip that is equal to the inverse of the rms noise of that strip. This is motivated from our measurements showing that although the rms noise and average X-ray signal may vary at the 20% level from strip-to-strip, their ratio is constant within errors. To first order, such uniformity is expected for charge sensitive amplifiers even if the open loop amplifier gain differs from channel-to-channel.

To find X-ray hits in the data, we search for strips having a pulse height greater than five sigma above the pedestal. A cluster is defined as that strip plus the neighboring two strips on either side. The distribution of total pulse height of the five strips, in units of the single channel rms noise, is shown in figure 6 for data taken with one of the 72 mm long detectors. Figure 7 shows the average pulse height of the strip with the largest signal in the cluster as well as the average pulse heights of its neighboring strips. The Gaussian fit to the data in figure 6 does not include points from the low energy tail of the distribution. This tail results from lower energy X-rays and events which occur near the edges of the amplifier integration period. The mean of the fitted curve is 13.3 sigma which extrapolates for minimum ionizing particles to a most probable energy loss that is 18.7 times the single channel noise. Assuming an electron-ion pair produced in silicon requires an average of 3.6 eV energy deposited, an equivalent noise charge of 1250 electrons is obtained which agrees within 10% of the expectation from figure 4 for a detector of 8.8 pF total strip capacitance (sum of strip-to-strip and strip-to-backplane capacitance). The standard deviation of the Gaussian curve in

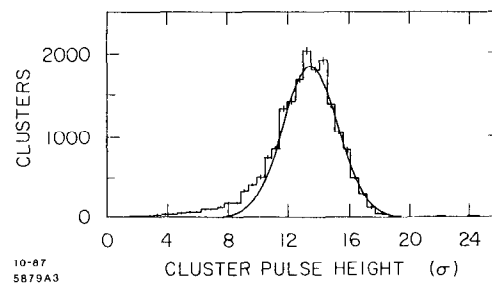
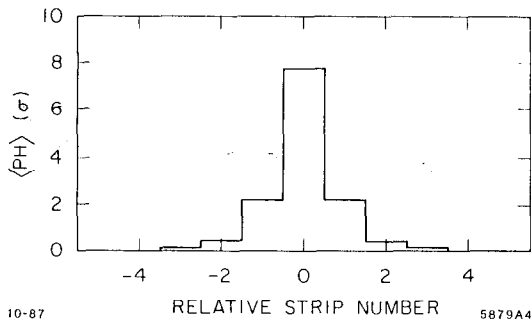


Figure 6. The distribution of the cluster pulse height in units of the single channel rms noise ( $\sigma$ ).



10-87 5879A4

Figure 7. The average pulse height of strips in the region of a cluster versus strip number. The strip with the largest pulse height is assigned a relative strip number of zero. The average pulse height is measured in units of the single channel rms noise ( $\sigma$ ).

figure 6 is about 20 % smaller than the naive prediction of  $\sqrt{5}$  sigma for independent channel-to-channel noise. However, it is consistent with our observation of a negative noise correlation of roughly .2 between neighboring channels that arises from the capacitive coupling of the strips.

#### Mechanical Support and Alignment

Since the spatial resolution of the modules will be  $\approx 5 \mu\text{m}$ , we need to know their locations to a much better precision. The general philosophy in the alignment procedure is to have the module support structure locate their positions only to a moderate accuracy while using other techniques to determine their precise location. The placement accuracy is set by the 2 mm  $z$  resolution of the central tracking chamber which translates into a  $r\phi$  uncertainty if the strips are not parallel to the  $z$  axis. We will place the modules to better than  $25 \mu\text{m}$  accuracy over their length so the  $r\phi$  uncertainty is less than  $1 \mu\text{m}$ .

The photo in figure 8 shows a prototype of one of two hemi-cylindrical structures that will house the modules. The inner shell of each hemi-cylinder has a three point suspension system which attaches to the beam pipe. The slots in the end-plates, which have been cut using electro-discharge machining, support the modules at each end. A spring fixture that is attached on each end of the module is compressed when inserted into the slots. Tests show that the resulting force keeps the radial and  $r\phi$  location of modules stable to within  $2 \mu\text{m}$  while allowing for a small  $z$  motion that prevents the bowing of the silicon detectors from the differential thermal expansion of the materials of the SSVD. The support structures will be fabricated out of aluminium except for the shells in the detector region which will be beryllium (250  $\mu\text{m}$  thickness).

The slot locations in the prototype endplates have been measured to be accurate to 15  $\mu\text{m}$ . As for the precise determination of the module locations, a method using a collimated X-ray beam is being considered. One would move the hemi-cylindrical structure by known amounts through a fixed beam and use the data read out from the modules to reconstruct their relative orientations. The X-rays will penetrate the materials of the modules and housing so the alignment can be done when the SSVD assembly is complete. Tests will begin shortly using a high power conventional X-ray tube to check whether this technique will give the required accuracy.

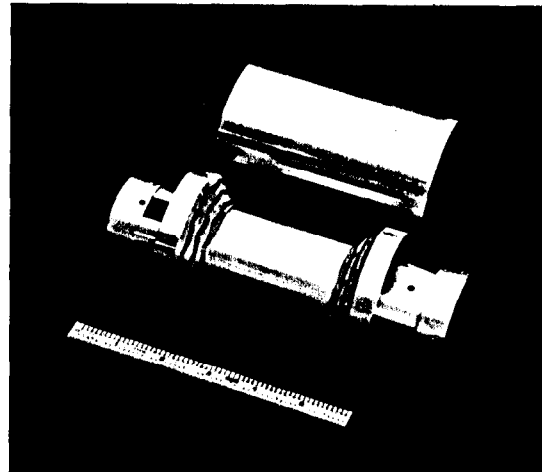


Figure 8. A photograph of the prototype mechanical support structure. The outer shell is shown detached from the inner shell and slotted endplate assembly.

After measuring the relative locations of the modules within each hemi-cylinder, they can be installed on the beam pipe in the Mark II where their alignment as a whole can be determined relative to the vertex drift chamber and central tracking chamber using tracks in the data. To monitor any movement of the beam pipe on which the SSVD is attached relative to the Mark II support structure which holds the other chambers, capacitive sensors [6] will be placed on extensions of the outer hemi-cylindrical shells of the SSVD. These will record  $r$ ,  $z$  and  $\phi$  displacements relative to ground pads that have been glued to the inner cylinder of the vertex drift chamber. Tests of individual sensors have given resolutions better than  $1 \mu\text{m}$  and a full mock-up of the detector interface region is now being built to verify that changes in the six degrees of freedom defining the relative orientation of the detectors can be unfolded with the required accuracy.

#### Summary and Outlook

We have successfully constructed SSVD prototype modules that are suitable for use in the Mark II. Currently, the final set of flexible cables, hybrids and detectors are being built in preparation for full assembly to begin early next year. One uncertainty that remains is whether the new fabrication of the Microplex chip will yield better radiation hardness. Basic measurements of the stability of the mechanical support structure have been made and attention is now turning more toward the alignment question. If things go according to plan, we should have the detector ready for installation in the Mark II by next summer.

#### References

- [1] Version 2 of the Microplex chip is described in G. Anzivino *et al.*, *Nucl. Instrum. & Methods A243*, (1986) 153.
- [2] The detectors described in the text were fabricated by Hamamatsu Photonics K.K., Hamamatsu City, Japan.
- [3] C. Adolpshen *et al.*, *Nucl. Instrum. & Methods A253*, (1987) 444.
- [4] M. Breidenbach *et al.*, *IEEE Trans. Nucl. Sci. NS-25*(1978) 706.
- [5] For details on the effect of radiation on Microplex 2 and 3, see the report by P. Dauncey *et al.*, from this conference.
- [6] The sensors are manufactured by Capacitec, Inc. of Ayer, Massachusetts.